ELSEVIER

Polymer 42 (2001) 6209–6219

polymer

www.elsevier.nl/locate/polymer

Poly(lactic acid): plasticization and properties of biodegradable multiphase systems

O. Martin, L. Avérous*

CERME: Materials and Packaging Research Centre (ESIEC), UMR INRA/URCA (FARE), B.P. 1029, 51686 Reims cedex 2, France

Received 25 October 2000; received in revised form 1 January 2001; accepted 22 January 2001

Abstract

Poly(lactic acid) (PLA) is a biodegradable aliphatic polyester well suited for disposable applications. PLA was plasticized with various biocompatible plasticizers. Their efficiency was evaluated in terms of glass transition temperature (T_g) shift and mechanical properties improvement. Significant decrease in T_g and rise in the elongation at break was obtained with polyethylene glycol and oligomeric lactic acid. Furthermore, PLA was melt-blended with thermoplastic starch (TPS). The properties of subsequent TPS/PLA blends were investigated through tensile and impact testing, thermal analysis (DSC), dynamic mechanical analysis and microscopy (SEM). From the mechanical results, low level of compatibility was found. The blends showed two distinct T_gs. However, the PLA phase varied toward the T_g of TPS with the blend composition, indicating some degree of interaction. Microscopic observations revealed non-uniformly dispersed PLA inclusions in the TPS matrix, confirming that phase separation has occurred.

Keywords: Poly(lactic acid); Plasticizer; Thermoplastic starch

1. Introduction

Poly(lactic acid) (PLA) has received much attention in the research of alternative biodegradable polymers [1–3]. PLA is a linear aliphatic thermoplastic polyester, produced from renewable resources and readily biodegradable [4,5]. PLAs are produced by ring-opening polymerization of lactides and the lactic acid monomers used are obtained from the fermentation of sugar feed stocks [6]. Generally, commercial PLA grades are copolymers of poly(L-lactic acid) (PLLA) and poly(D,L-lactic acid) (PDLLA), which are produced from L-lactides and D,L-lactides, respectively. The ratio of L- to D,L-enantiomers is known to affect the properties of PLA, such as the melting temperature and degree of crystallinity. To date, PLA resins have mostly been used for biomedical applications such as drug delivery systems [7]. Thanks to mechanical properties comparable to those of polystyrene, PLA could reasonably substitute conventional polymers in domains such as packaging. However, the low deformation at break and quite elevated price of PLA limit its applications.

Considerable efforts have been made to improve the properties of PLA so as to compete with low-cost and flexible commodity polymers. These attempts were carried out either by modifying PLA with biocompatible plasticizers, or by blending PLA with other polymers. Varying types of chemicals, such as citrate esters, have been tried to plasticize PLA [8]. Recently, plasticizers such as poly(ethylene glycol) (PEG), glucosemonoesters and partial fatty acid esters [9,10] were used to improve the flexibility and impact resistance of PLA. The resulting plasticized PLA materials gained in deformation and resilience. None of these studies proposed oligomeric lactic acid (OLA) and glycerol as plasticizers for PLA.

Blends of PLA with various non-biodegradable polymers have been investigated [11–13]. Biodegradable blends of PLA with other aliphatic polyesters such as poly(ε-caprolactone) [14–16], poly(butylene succinate) [17,18] and poly(hydroxy butyrate) [19,20] were also reported in the literature. Some of these blends were found to be immiscible, resulting in fairly poor mechanical properties. Surprisingly, none of these studies have investigated the use of thermoplastic starch (TPS) as the biodegradable blend component for PLA, although it offers unquestionable advantages in terms of cost and sustainability. TPS has been widely used in association with other polyesters because of its low cost, satisfactory properties, renewability and biodegradability. Blends of TPS with

* Corresponding author. Tel.: +33-3-26-913-914; fax: +33-3-26-913-803.

E-mail address: luc.averous@univ-reims.fr (L. Avérous).

0032-3861/01/$ - see front matter
PII: S0032-3861(01)00086-6

Table 1
Properties of the plasticizers used in the study (nd means that the characteristics were not determined)

Commercial name	Designation	M_w (g/mol)	Density	Boiling point (°C) at 760 mm Hg
Glycerol	GLYC	nd	1.26	182
Citrate ester	CITRO	360	nd	nd
Polyethylene glycol	PEG1500	1500	1.15	280
Polyethylene glycol	PEG400	400	1.13	260
PEG monolaurate	M-PEG	400	0.98	260
Oligomeric lactic acid	OLA	nd	1.20	nd

PCL [21], polyesteramide [22] and PHBV [23] have been reported. Some starch-based blends have been commercialized like Mater-Bi [24] (Novamont — Italy) or Bioplast [25] (Biotec — Germany).

In this study, we have investigated the influence of plasticizers such as PEG of various kinds, citrate ester (CITRO), OLA and glycerol on the physical properties of PLA. Moreover, we have blended thermoplastic wheat starch together with PLA. The properties of the subsequent materials were characterized through tensile testing, thermal and thermomechanical analysis and microscopy. The efficiency of the plasticizers as well as the compatibility of the TPS/PLA blends are discussed.

2. Experimental

2.1. Materials

The PLA was obtained from Cargill-Dow, and consists of 92% L-lactide and 8% meso-lactide contents. The average molecular weight of 49,000 was determined by intrinsic viscosity measurements in chloroform at 25°C. The PLA pellets were transparent and amorphous, with a glass transition temperature of 58°C. The plasticizers selected for the study were purchased from Sigma. The choice of these plasticizers was based on requisites such as non-toxicity and biocompatibility. Their characteristics are listed in Table 1. Wheat starch was purchased from Chamtor (France). The starch contains 74% amylopectin (branched component) and 26% amylose (linear carbohydrate polymer). The residual protein is less than 0.2%. Glycerol with a 99.5% purity was used as processing aid and plasticizer of TPS.

2.2. Material preparation

2.2.1. PLA plasticization

PLA was plasticized according to a two-step procedure. The pellets were first dried in a vented oven at 40°C overnight prior to processing. Varying amounts of each plasticizer (10 and 20, in wt%) were then mixed together with PLA pellets within a Brabender mixing chamber for 15 min at 90°C. In a second step, each polymer–plasticizer system was extruded with a single-screw extruder (SCAMIA S2032, France), equipped with a specific high-shear zone (conical-shaped element). Finally, a DK Codim NGH 50/100 injection-molding machine (France) with a clamping force of 50 tons was used to obtain standard tensile bars. Temperature settings ranged from 120 to 180°C, and the holding pressure and time were 800 bars and 20 s, respectively. The injection-molded specimens were 10 mm wide and 4 mm thick (French standard NFT 51-034 1981).

2.2.2. TPS/PLA blends preparation

Three types of TPS have been chosen, differing in the glycerol/starch ratios, in order to modulate the materials properties. Table 2 shows the different TPS formulations used in the study in terms of starch, water and glycerol contents, plus the densities. The properties of TPS are dependent on the amount of plasticizer used. Thus, the TPS1 formulation (the lower glycerol/starch ratio of 0.14) is a rigid and brittle material, whereas TPS2 and TPS3 (with ratios of 0.26 and 0.54, respectively) are flexible materials. The different TPS pellets were conditioned at 65% RH for 8 days prior to blending, in order to reach moisture equilibrium. TPS and PLA pellets were then melt-blended in various proportions with the single-screw extruder equipped

Table 2
TPS formulations used in the study and density of the injection-molded materials

Material	Starch content[a]	Water content[a]	Glycerol content[a]	Glycerol/starch ratio[a]	Density
TPS1	74	16 (8.5)	10 (11)	0.14 (0.14)	1.39
TPS2	70	12 (8.7)	18 (18)	0.26 (0.25)	1.37
TPS3	65	0 (12.6)	35 (30)	0.54 (0.50)	1.34
PLA	–	–	–	–	1.25

[a] The starch, water and glycerol contents are given in wt% (wet basis), and values given in brackets are the glycerol and water contents or glycerol/starch ratio determined after processing.

with a conical-shaped element. The subsequent extrudates were pelletized and then reconditioned (at 65% RH) prior to injection molding. The DK Codim NGH 50/100 injection-molding machine was used to shape the blends into standard tensile bars. A temperature profile ranging between 120–180°C was set along the screw barrel. Optimal holding pressure and time were 1000 bars and 20 s, respectively. Injection-molded parts were shaped into dumbbell specimens (NFT 51-034 1981).

2.3. Characterization

2.3.1. Tensile testing

Tensile testing was carried out on an Instron tensile testing machine (model 4204) according to the ASTM D882-91, with a crosshead speed of 50 mm/min. The gauge length was adjusted for each blend composition (around 100 mm), and each sample's width and thickness were measured before testing. Ten samples for each blend composition were tested after a 6 week conditioning period at 50% RH and 23°C. Young's modulus, maximum tensile strength and elongation at break (EB) were obtained using Instron series 4 software.

2.3.2. Impact resistance

The impact resistance was determined with an impact tester (JPS, France) according to the Charpy method (French standard NFT 51-035 1983). Ten samples (without notch) conditioned like the tensile test specimens were cut out from the central part of the dumbbell specimens (dimensions $60 \times 10 \times 4$, in mm) and tested for each blend composition. A 4 J pendulum was used.

2.3.3. Thermal analysis

Differential scanning calorimetry (M-DSC 2920, TA instruments, USA) was used for the thermal analysis of PLA and blends. The pure and plasticized PLA samples were sealed in aluminum pans (10 mg) and heated from 25 to 200°C at a rate of 10°C/min, held at that temperature for 1 min, then air cooled to 25°C (cooling rate of 25°C/min) before a second heating scan from 0 to 200°C at 10°C/min scan rate. A nitrogen flow (50 ml/min) was maintained throughout the test. TPS/PLA blends were sealed in hermetic aluminum pans to prevent water volatilization from the starch component. Blend samples were first heated from 25 to 100°C at a rate of 10°C/min. The samples were kept at 100°C for 10 min, air cooled to 25°C and heated again from −100 to 200°C at 10°C/min. The glass transition temperature (T_g), crystallization temperature (T_c), melting temperature (T_m) and degree of crystallinity (X_c) were determined from the second heating scans. The first scan was meant to discard thermal history of the samples. The T_m and T_c were taken at the peak value of the respective endotherms and exotherms, and the T_g at the mid-point of heat capacity changes. When multiple endothermic peaks were found, the peak temperature of the main endotherm was taken as T_m. The degree of crystallinity of the samples meant for mechanical and DMA analyses, measured from the first heating scans, were similar to those of second heating scans.

2.3.4. Thermo-mechanical analysis

Dynamic mechanical analysis (DMA) was carried out on a DMA 2980, TA instrument, USA. Test bars were cut from the tensile bar specimens (dimensions $W \times H \times L = 10 \times 4 \times 70$, in mm) and mounted on a dual-cantilever geometry. The temperature used in the experiments ranged from −100 to 160°C, at a heating rate of 1.5°C/min. The strain was set at 14.5 μm, with a frequency of 1 Hz. The TPS and TPS/PLA test samples were coated with silicon grease in order to avoid water volatilization during the test. Storage modulus (E'), loss modulus (E'') and tan δ were recorded as a function of temperature.

2.3.5. Scanning electron microscopy

Scanning electron microscopy (SEM) was performed on selected TPS/PLA blends with a Philips SEM515 scanning electron microscope. The blend samples were cut with a diamond precision saw, then polished with a non-aqueous solvent and finally etched with chloroform (99.5% purity) for 24 hours to remove the PLA phase, to reveal morphology of the blend. Low voltage (2.1 kV) was used, and the samples were not coated.

3. Results and discussion

3.1. Effect of various plasticizers on PLA

3.1.1. Thermal properties

The results obtained from differential scanning calorimetry of PLA and plasticized PLA are shown in Table 3. The pure PLA shows a clear glass transition at 58°C, and a very small melting endotherm at 152°C, corresponding to residual crystallinity. The crystallization behavior of PLA was checked through isothermal crystallization from the melt at 110°C, for various time intervals. As shown in Fig. 1, the crystallinity increases with increasing isothermal time intervals, and the heat capacity (ΔC_p) decreases accordingly. The degree of crystallinity seems to reach a maximum of 34% around 30 min of isotherm at 110°C [26]. In the meantime, the heat capacity gradually decreases from 0.48 to a minimum of 0.23 J/g/°C. That decrease in heat capacity change is a direct result of reducing amorphous domains, due to crystalline growth. The crystallization behavior of PLA has been discussed elsewhere, and indicates that crystallinity can be obtained either after annealing at 105°C for 90 min [18], or at a cooling rate from the melt inferior to 4°C/min [26]. It may be stated that under standard processing conditions, PLA may remain mainly amorphous because of its slow crystallization kinetics. Moreover, the air cool applied in the DSC cell to

Table 3
Thermal and mechanical properties of plasticized poly(lactic acid) (standard deviations are given in brackets)

Material	T_g (°C)	T_c (°C)	T_m (°C)	Crystallinity (%)	E modulus (MPa)	EB (%)
Pure PLA	58	no	152	1	2050 (44)	9 (2)
Glycerol						
10%	54	114	142	24.3	–	–
20%	53	110	141	25.4	–	–
CITRO						
10%	51	no	144	12	–	–
20%	46	no	142	20	–	–
M-PEG						
10%	34	94	148	22	1571 (51)	18 (2)
20%	21	75	146	24	1124 (33)	142 (19)
PEG1500						
10%	41	105	152	17	–	–
20%	30	85	148	25	–	–
PEG400						
10%	30	82	147	26	1488 (39)	26 (5)
20%	12	67	143	29	976 (31)	160 (12)
OLA						
10%	37	108	144	21	1256 (38)	32 (4)
20%	18	76	132	24	744 (22)	200 (24)

PLA samples (cooling rate of 25°C/min) between each heating scan do not allow additional crystallization.

Table 3 shows the glass transition temperatures (T_g) of plasticized PLA systems, as well as crystallization and melting temperatures (T_c and T_m). Compared to pure PLA which solely shows a sharp T_g, the addition of a plasticizer to the PLA induces crystallization (T_c), and thus fusion (T_m). This behavior is typical of plasticized thermoplastics, where plasticizers may promotes crystallinity due to enhanced chain mobility. Interestingly, most melting endotherms show two distinct peaks, as shown in Fig. 2. Few authors [11] have reported this behavior as a result of lamellar rearrangement during crystallization of PLA: a 'shoulder' or low-temperature peak is formed on the melting endotherm of the original crystallites. Besides, the different crystalline structures that can exist in PLA have been described by Cartier et al. [27]. As shown in Table 3, plasticized PLA systems show a single T_g, lower than that of

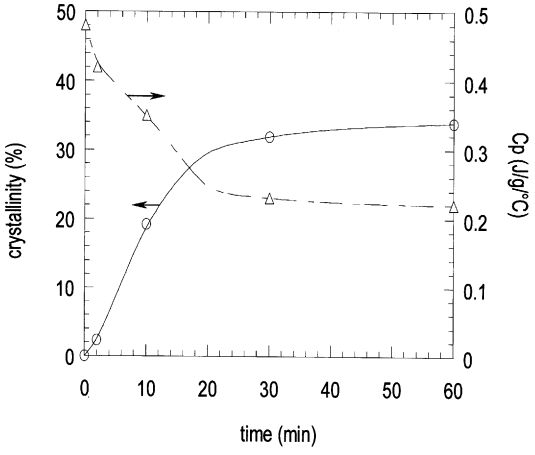

Fig. 1. Crystallinity (straight line) and heat capacity increase (dashed line) of PLA films as a function of the isothermal conditions.

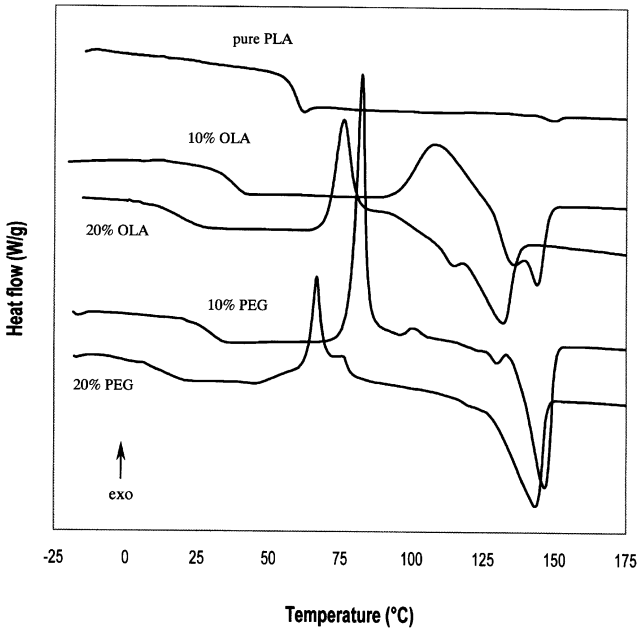

Fig. 2. DSC traces of pure and plasticized PLA (plasticizers used are OLA and PEG400).

pure PLA, which was found to decrease with increasing plasticizer content. The amplitude of T_g depression lies between 58°C (T_g of pure PLA) and the ambient temperature. The lower T_g values of 12 and 18°C, were obtained with PEG400 and OLA, respectively. A significant decrease in the melting temperature (T_m) of 10 to 15 °C was also observed, and the depression of T_m did not seem to be much dependent on the plasticizer concentration. In the meantime, the degree of crystallinity was seen to increase. The calculation of the degree of crystallinity is based on the enthalpy of fusion of 100% crystalline PLA, equal to 93 J/g [28]. Besides, the crystallization temperature (T_c) was seen to decrease with increasing plasticizer content, which is consistent with the fact that PLA crystallizes with more ease at lower temperatures due to enhanced chain mobility as the plasticizer level increases. The M-PEG plasticizer led to similar results to that of PEG400, except that T_g shifts were not as pronounced. The other plasticizers had only limited effect on the thermal transitions of PLA, especially glycerol that induced a T_g shift as low as 5°C (from 58 to 53°C), even at 20% loading. Glycerol is clearly a non-plasticizer of PLA. However, similarly to the other plasticizers, the addition of glycerol also favored crystallization around 110°C. The thermal characteristics of plasticized PLA compared to pure PLA demonstrated that PEG400 and OLA can be regarded as the most efficient plasticizers of PLA.

3.1.2. Mechanical and thermo-mechanical properties

Young's elasticity modulus (E) and EB were determined for pure PLA and selected plasticized PLA systems, as shown in Table 3. PLA is a high modulus (2 GPa) and brittle material. Its EB is as low as 9%. As expected, the addition of plasticizers caused substantial decrease in the Young's modulus of plasticized materials. The decrease in modulus ranged from 28 to 65% according to the type and level of plasticizer used. The higher moduli reductions of 53 and 65% were obtained at 20% of added PEG400 and OLA, respectively. In the meantime, the EB increased with increasing plasticizer concentration. An EB as high as 200% was obtained, indicating that the properties of PLA can easily be tuned from rigid to ductile.

The efficiency of the plasticizers was also appraised through DMA. The influence of a plasticizer (PEG400) on the storage modulus (E') and dissipation factor tan δ of the PLA is shown in Fig. 3. The DMA curve of pure PLA shows a marked drop in E' and a sharp tan δ peak around 67°C, corresponding to the glass transition. The rise of E' around 100°C is due to crystallization. Above T_g, the increase of chain mobility favors the crystallization process, which proceeds thanks to a slow scan rate (1.5°C/min) and sinusoidal solicitation. By interrupting the DMA run of pure PLA at 125°C (i.e. at the maximum of the E' rise), it was checked that the crystallinity reached up to 29%. Finally, as the temperature increases, the storage modulus drops again as the material starts to flow. The DMA curves of plasticized

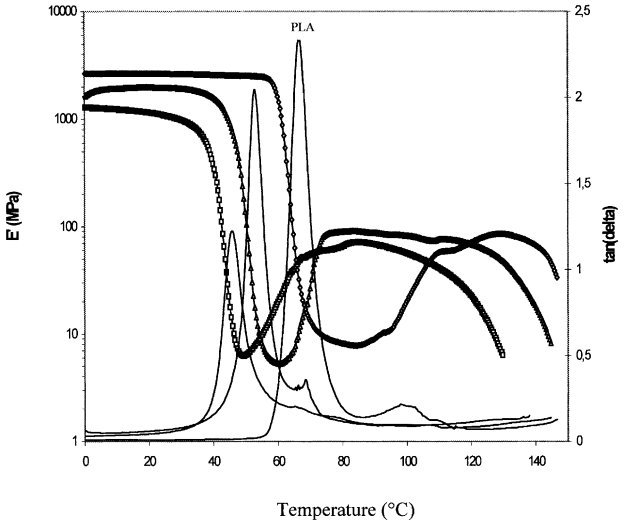

Fig. 3. Storage modulus and tan δ (DMTA) of pure and plasticized PLA systems (◇, pure PLA; △, PLA with 10% PEG400; □, PLA with 20% PEG400). Each tan δ peaks associated with the α-relaxation are located at respective modulus drops.

PLA are of similar shape. The E' below T_g shows only a slight dependence on the composition. The modulus drop associated with the T_g of plasticized PLA decreases almost linearly with increasing plasticizer concentration, from 67°C for pure PLA to 54 and 46°C for a PEG concentration of 10 and 20%. Moreover, the height of tan δ peak decreases accordingly. This phenomenon has been previously dealt with [18], and the explanation lies in the degree of crystallinity: amorphous PLA shows a very sharp and intense peak because there is no restriction to the chain motion, whereas the crystallinity of plasticized PLA test samples hinder the chain mobility, resulting in the reduction of sharpness and height of tan δ. The rise of E', due to crystallization, still proceeds for the plasticized PLA test bars, but at lower temperatures than for pure PLA.

3.2. Characterization of TPS/PLA blend properties

Various TPS (see Table 2) were melt-blended together with PLA in an extruder. The reader is kindly requested to refer to previous studies [21,22] to get more detail on the formulations and mechanical behavior of TPS.

3.2.1. Mechanical properties

The mechanical properties (modulus, tensile strength, EB and impact resistance) of TPS/PLA blends, as well as those of pure components, are shown in Table 4. When looking at the characteristics of pure TPS and pure PLA (composition 100/0 and 0/100, respectively), two kinds of behavior are observed. PLA and TPS1 are high modulus and low EB materials. Inversely, TPS2 and TPS3 are low modulus and highly deformable materials, especially for the TPS3 type. As for the subsequent blends, it can be clearly seen that the

Table 4
Mechanical properties of TPS/PLA blends (standard deviations are given in brackets)

Blend ID	Composition (w/w)	*E* Modulus (MPa)	Tensile strength (MPa)	EB (%)	Impact resistance (kJ/m^2)
TPS1/PLA	100/0	1071 (31)	19.5 (1.8)	2.8 (0.6)	0.7 (0.1)
	90/10	1318 (27)	14.1 (1.3)	1.3 (0.1)	0.3 (0.1)
	75/25	1439 (56)	12.0 (1.8)	0.9 (0.1)	0.2 (0.1)
	60/40	1527 (30)	11.2 (1.6)	0.8 (0.1)	0.4 (0.1)
	25/75	1850 (35)	30.2 (1.6)	2.9 (0.2)	1.7 (0.1)
	0/100	2050 (44)	68.4 (1.1)	9.4 (1.4)	11.9 (2.3)
TPS2/PLA	100/0	82 (1)	3.4 (0.1)	152.0 (13.0)	No break
	90/10	170 (8)	2.9 (0.1)	48.8 (8.0)	3.4 (1.1)
	75/25	378 (30)	4.8 (0.3)	5.7 (1.8)	1.1 (0.3)
	60/40	718 (38)	12.1 (2.0)	2.1 (0.3)	1.8 (0.3)
	0/100	2050 (44)	68.4 (1.1)	9.4 (1.4)	11.9 (2.3)
TPS3/PLA	100/0	20 (2)	1.9 (0.1)	112.0 (4.2)	No break
	90/10	53 (1)	1.4 (0.1)	35.7 (1.0)	No break
	75/25	129 (12)	2.8 (0.2)	6.4 (0.4)	6.6 (1.2)
	60/40	346 (18)	5.3 (0.2)	1.7 (0.1)	1.7 (0.2)
	25/75	1456 (36)	30.3 (1.2)	3.1 (0.3)	2.4 (0.3)
	0/100	2050 (44)	68.4 (1.1)	9.4 (1.4)	11.9 (2.3)

elastic modulus ranges between those of the pure components, whatever the TPS type. Simple models [29] can describe the change of modulus with composition. The modulus of polymer blends theoretically lies between an upper limit given by the parallel model (or Reuss model):

$$E = \phi_1 E_1 + \phi_2 E_2 \quad (1)$$

and a lower limit given by the series model (Voigt model):

$$1/E = \phi_1/E_1 + \phi_2/E_2 \quad (2)$$

where E_i and ϕ_i are, respectively, the modulus and volume fraction of the *i*th phase.

In Fig. 4, the Young moduli of TPS1/PLA (a) and TPS3/PLA (b) blends are plotted as a function of the volume fraction of PLA, and compared with the parallel and series model. In the case of TPS1-based blends, the experimental moduli are superior to the upper limit, whereas the moduli of TPS3-based blends range between the two limits. Furthermore, the moduli of TPS3-based blends show excellent agreement with the Davies model [29]: this latter model assumes co-continuity and homogeneity of the blend. The equation is given by:

$$E^{1/5} = \phi_1 E_1^{1/5} + \phi_2 E_2^{1/5} \quad (3)$$

The moduli of TPS2-based blends are not presented. They show an intermediate behavior, with experimental values closer to the parallel model. Apart from some changes in the modulus dependence on the composition of blend, all TPS/PLA blend series follow more or less the classical rule of mixtures. The EB and impact resistance of these blends did not follow the same trend. In fact, all blends show a marked decrease in the EB, tensile strength and impact resistance, as shown in Fig. 5. The curves are seen to deviate negatively from the classical additivity rule, in the whole composition range. Many EB and tensile strength data are even inferior to that of pure constituents, at PLA content as low as 10% (wt%) for TPS1-based blends, and 25% for TPS2- and TPS3-based blends. Similarly, blends show a marked decrease in the impact resistance. The TPS2 and TPS3 materials, which have elevated impact resistance (no break), broke upon impact at PLA concentrations of 10 and 25%, respectively. There is no explanation for that decreased ability to hold deformation (both in the EB and impact resistance) except that the PLA phase forms immiscible dispersions within TPS, leading to a strong weakening effect. Finally, it is interesting to note that the PLA-rich blends (composition 25/75) did not show better performances in that both the EB and impact resistance were lower than that of pure PLA, i.e. 3 versus 9% for the EB and 2 versus 12 kJ/m^2 for the impact resistance. The fairly bad mechanical properties of TPS/PLA blends may be explained in terms of lack of affinity between the two phases. But, this result alone is not absolute evidence of non-compatibility.

3.2.2. Thermal properties

The thermal characteristics of TPS/PLA blends were determined by DSC. The thermal transitions of blends are useful in that they reveal the interactions between respective polymers [30,31]. Practically, in a binary polymer blend, some level of compatibility may be inferred when the two observed T_gs are shifted toward each other.

The glass transition temperatures of TPS1, TPS2 and TPS3 are 43, 10 and −20°C, respectively [22]. The T_g of pure PLA is about 58°C. The DSC thermograms of TPS2/PLA blends are shown in Fig. 6. The T_g value of PLA is slightly dependent on the blend composition, indicating that the binary blend is partially miscible. The T_g of PLA actually decreased from 58°C for pure PLA to 53, 51, 50 and 47°C for PLA contents in blends of 75, 40, 25 and 10%,

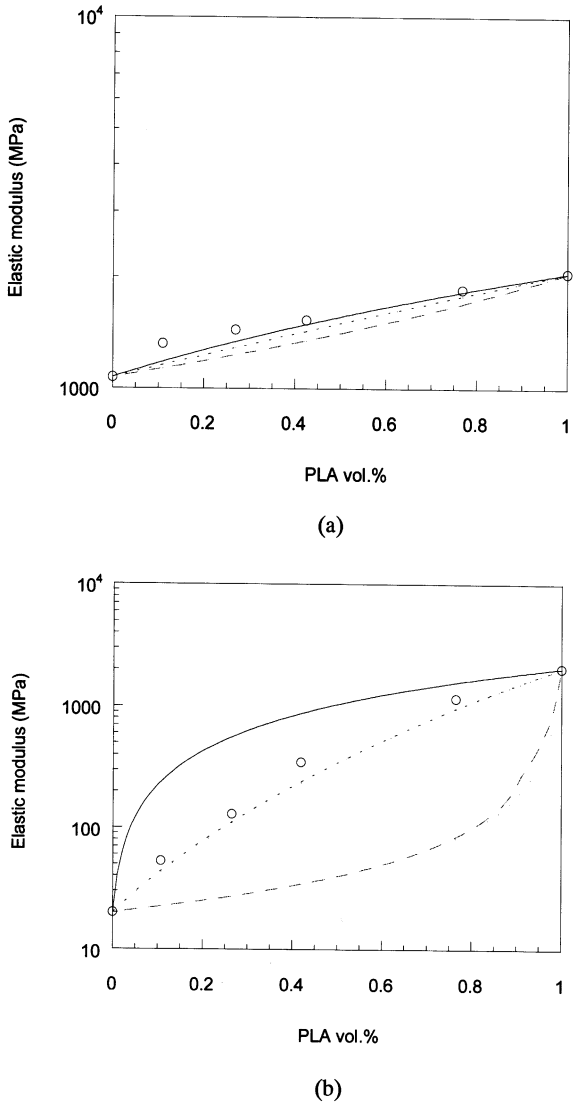

Fig. 4. Experimental Young moduli of TPS1/PLA (a) and TPS3/PLA (b) blends compared with the parallel (straight line), series (long-dash line) and Davies (short-dash line) models.

respectively. The T_g decreased gradually as the content of TPS in the blend increased. In the meantime, the T_g of TPS seems to be shifted toward higher temperatures as the PLA content increases. However, the T_g transitions of TPS were difficult to determine, whatever the blend composition.

The PLA melting peak, which is very small in pure PLA, reappears in the blends. As shown in Fig. 6, the temperature of PLA melting peak shows a shift toward lower temperatures as its proportion in the blend decreases. It actually decreased from 148°C for the 25/75 composition (75% PLA) to 139°C for the lower PLA concentration (10% PLA). The T_m value of pure PLA is 152°C. Two hypotheses may be inferred to explain that phenomenon. Firstly, a depression in T_m is typically observed when a semi-crystalline component (PLA) is miscible with an amorphous polymer (TPS in our

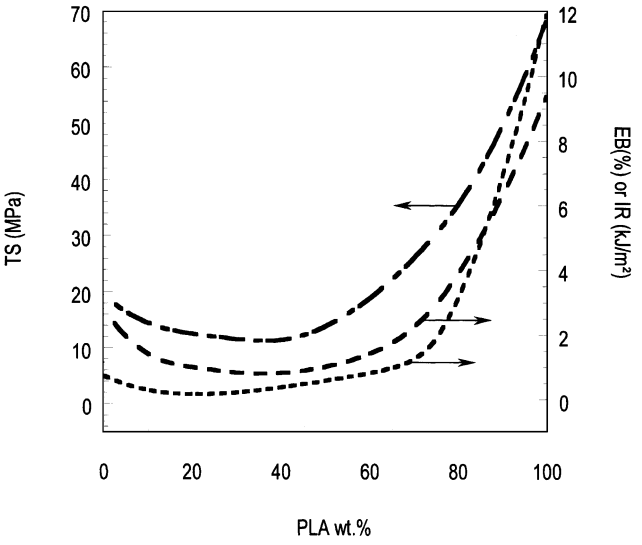

Fig. 5. Mechanical properties of TPS1-based blends as a function of PLA concentration. Tensile strength (TS) is the long-dash line, EB is the medium dash-line and the impact resistance (IR) is the short-dash line.

case). Because the depression is moderate, a small degree of miscibility between the blend components may be concluded. Moreover, no significant change in the crystallinity of the PLA phase was noticed among the blends. Secondly, the influence of glycerol on the PLA phase cannot be discarded. If glycerol has a negligible influence on the T_g of PLA (Table 3), it actually reduces the melting temperature of PLA from 152 to 142°C, at a glycerol concentration of 10%. The gradual decrease of T_m with increasing TPS content may confirm that glycerol plays a significant role.

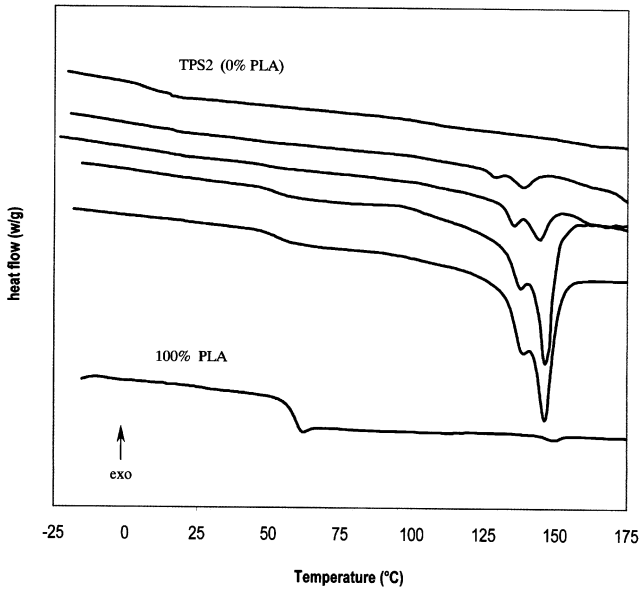

Fig. 6. DSC traces of TPS2-based blends (from top to bottom 0, 10, 25, 40, 75 and 100 wt% of PLA).

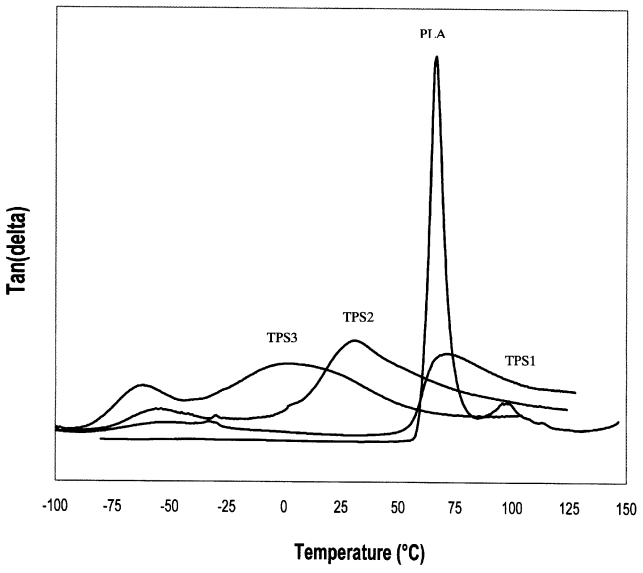

Fig. 7. Tan δ curves (DMTA) associated with the glass transition of TPS1, TPS2, TPS3 and PLA.

3.2.3. Thermo-mechanical analysis

DMA experiments were carried out on most TPS/PLA blend series, plus pure components. The tan δ of TPS and PLA are shown in Fig. 7. The α-relaxation processes associated with the glass transition of the amorphous phase of TPS and PLA could be clearly determined. The α-relaxation temperatures (T_α), taken at the maximum of respective tan δ peaks, were 72, 31 and 2°C for TPS1, TPS2 and TPS3, and 67°C for PLA. Again, the T_α of TPS is seen to decrease with increasing glycerol content in the starch. As expected, the T_α values associated with the glass transition of TPS and PLA differ significantly from the T_g results found by DSC [21]. A secondary transition (β-relaxation) is observed between −54 and −63°C, attributed to the glass transition of glycerol [22].

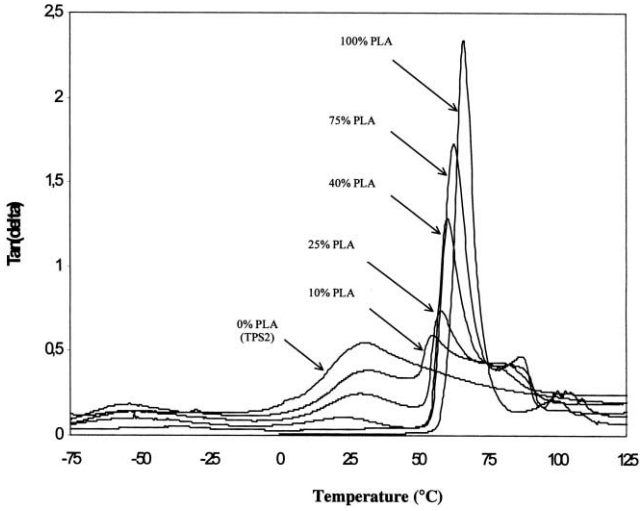

Fig. 9. Tan δ (DMTA) curves associated with the glass transition of each phase of the TPS2/PLA blends.

The storage modulus and tan δ curves of TPS2/PLA blends are shown in Figs. 8 and 9. For each blend composition, three relaxation processes could be distinctively identified, associated with the transition of each blend phase. The low temperature transition associated with the relaxation of glycerol is visible between −50 and −65°C, especially for the higher TPS contents. Around 30°C, the modulus drop and tan δ peak can be associated with the glass transition of TPS2, and the high temperature transition (around 70°C) can be attributed to the glass-to-rubber transition of PLA. The storage modulus and tan δ curves of TPS3/PLA blends are also shown in

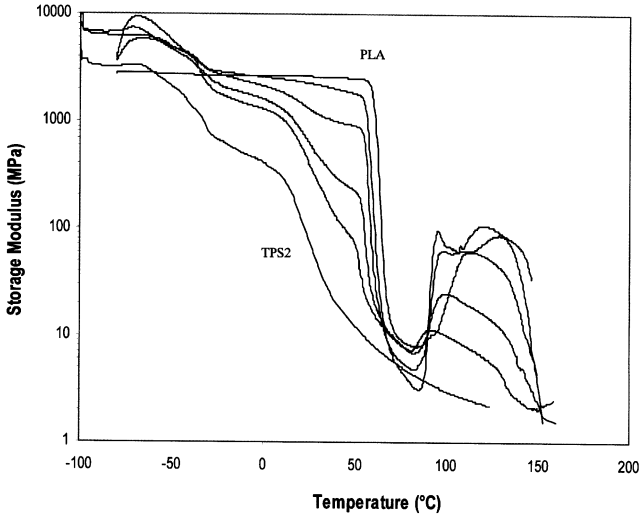

Fig. 8. Storage modulus (E') curves (DMTA) of TPS2/PLA blends (from top to bottom 100, 75, 40, 25, 10 and 0 wt% PLA).

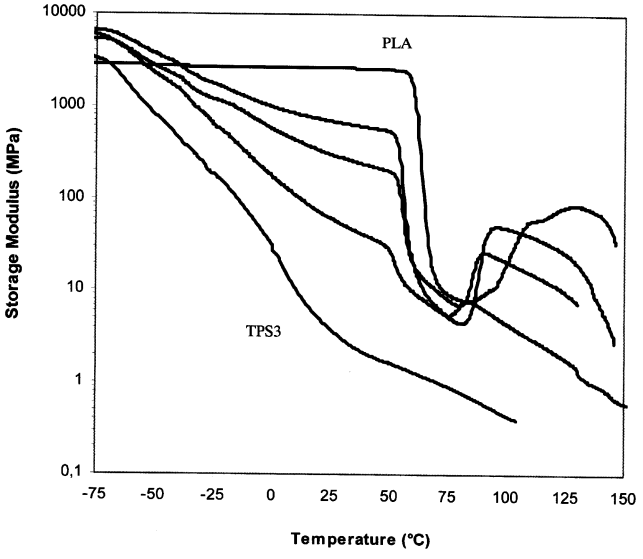

Fig. 10. Storage modulus (E') curves (DMTA) of TPS3/PLA blends (from top to bottom 100, 40, 25, 10 and 0 wt% PLA).

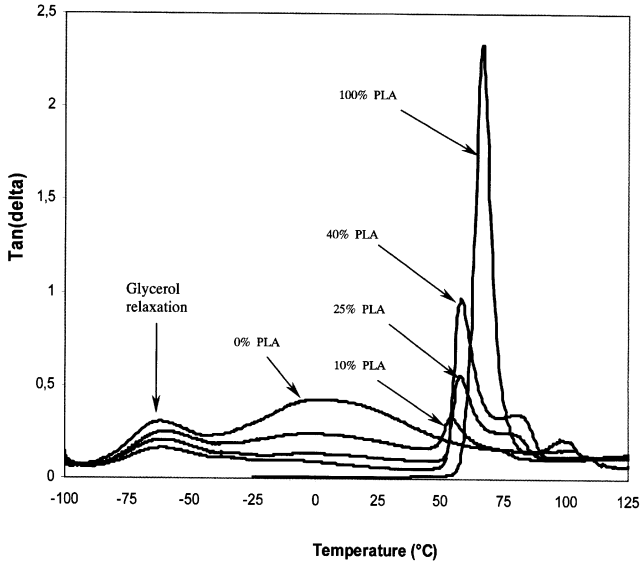

Fig. 11. Tan δ curves (DMTA) associated with the glass transition of each phase of the TPS3/PLA blends.

Figs. 10 and 11. They show exactly the same behavior than TPS2-based curves, with the TPS3 glass transition located around 0°C. Table 5 presents the α-relaxation temperatures (T_α) associated with the glass transitions of each blend phase of the TPS2/PLA and TPS3/PLA blends. The temperature shift between the T_α of pure components and T_α of each blend phase can be clearly seen. The T_α of the PLA phase show gradual decrease with increasing amounts of TPS. In particular, the T_α of the PLA phase decreased from 67°C (pure PLA, composition 0/100) to 55 and 54°C in the 90/10 blend composition of TPS2/PLA and TPS3/PLA, respectively. The change in T_α over the whole composition range indicates that there is some interaction between TPS and PLA. As a result, partial miscibility may be inferred. Unlike DSC, the influence of glycerol on PLA may be excluded because we have seen that glycerol has a limited effect on the glass transition of

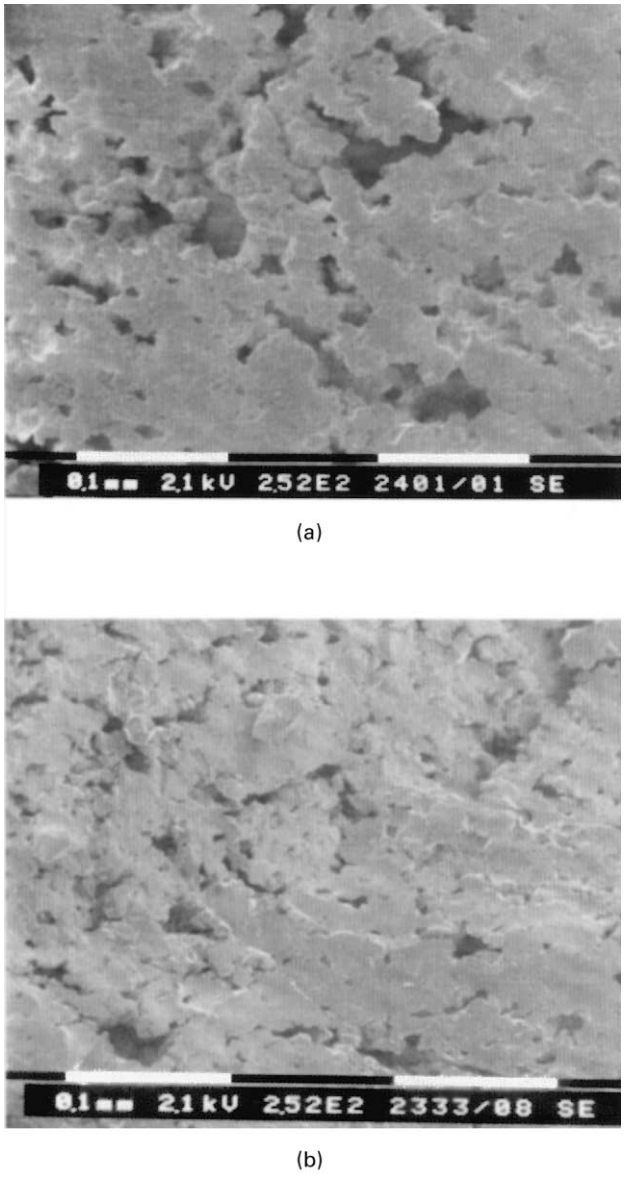

Fig. 12. SEM images of TPS1/PLA (a) and TPS3/PLA (b) with a blend composition of 75/25 (w/w). The scale bar is 100 μm.

Table 5
Temperatures of the α-relaxation associated with the glass transition of each blend phase (i.e. T_α of the TPS phase and PLA phase, respectively) (T_α are taken at maximum of tan δ peak; n.v. means non-visible)

	TPS2/PLA blends		TPS3/PLA blends	
Composition (w/w)	T_α (TPS) (°C)	T_α (PLA) (°C)	T_α (TPS) (°C)	T_α (PLA) (°C)
100/0	31.4	–	2.4	–
90/10	32.7	55.5	1.1	54.2
75/25	30.1	58.6	n.v.	57.6
60/40	27.2	60.6	n.v.	58.5
25/75	n.v.	63.1	–	–
0/100	–	66.9	–	66.9

PLA. Finally, the rise of E' between 80 and 125°C is also observed in blends: crystallization of the PLA phase proceeds during DMA runs (low scan rate, sinusoidal solicitation) correlates well with the results obtained in DSC. The amplitude of the E' increase is directly dependent of the amount of PLA in the blends.

The DMA curves of TPS1/PLA are not presented because they do not show distinct relaxations due to overlapping of the TPS1 and PLA transitions (67 and 72°C, respectively). Finally, it should be underlined that the storage modulus E' of TPS/PLA blends (for both TPS2 and TPS3) below T_α strongly depends on the composition. The storage modulus of blends below T_α is significantly higher than that of pure TPS, even at the lower PLA concentrations (see Fig. 8). That effect is even more pronounced on TPS3 (see Fig. 10). Therefore, the flexible TPS3 matrix is significantly reinforced by introduction of 10 or 25% dispersed PLA phase.

3.2.4. Blend morphology

The morphology of TPS/PLA blends was analyzed thanks to a scanning electron microscope. The areas where PLA was removed appear as dark holes. Fig. 12 shows the phase distribution of TPS1/PLA (a) and TPS3/PLA (b) with a blend composition of 75/25 (w/w). In both cases, the SEM images show large and non-uniform holes, suggesting that TPS forms a continuous phase and PLA a separated coarse phase [32]. Smaller holes however, were observed in Fig. 12b, which is a result of a finer dispersion (average size of 10–20 μm versus 40–60 μm). Because the phase separation of our blends is obvious, they may be classified as rather incompatible. It shall be pointed out that incompatible blend systems generally show complex phase morphologies, dominated by relative shear-viscosity and interfacial tension of the respective polymer melts [33]. High melt-viscosity differentials may yield coarse phase morphology. According to Biresaw and Carriere [34], the interfacial energy results, based on surface energy measurements, predicts low compatibility between starch and PLA. The morphologies observed correlate well with the mechanical behavior, in that the introduction of an immiscible phase to a more or less ductile polymer matrix drastically diminishes the mechanical properties (tensile strength, EB and impact resistance).

4. Conclusions

PLA is a promising biodegradable polymer. However, because of its inherent brittle behavior, we have blended it with various low-molecular weight plasticizers. The efficiency of respective plasticizers was investigated through DSC and mechanical determinations. Glycerol was found to be the least efficient plasticizer. Thermal analyses demonstrated that OLA and the lower molecular weight PEG (PEG400) gave the best results. The glass transition temperature decreased from 58 to 12°C and 18°C for 20 wt% of PEG400 and OLA, respectively. Thermal analysis also revealed a non-negligible depression of the melting point temperature of about 10–15°C. The elastic modulus was seen to decrease as the concentration of plasticizer increased. In the meantime, EB reached up to 200% in the range of concentration tested.

We have also investigated the properties of PLA blended with TPS. The properties and compatibility of these biodegradable polymer blends were determined through mechanical, thermal and dynamic testing. A dependence of PLA glass transition temperature on the blend composition was observed through DSC and DMA, indicating a small degree of compatibility between the blend components. However, the mechanical characteristics of the blends decreased drastically, even at the lower PLA contents (i.e. 10 and 25 in wt%). In particular, the EB and impact resistance of blends reached values lower than that of pure components. One may conclude the introduction of a non-compatible component to a more or less ductile matrix (TPS1 or TPS3) usually provokes dramatic loss in the mechanical properties. In the present work, the TPS matrix was transformed into a brittle material when a dispersed phase of PLA was added. The SEM micrographs performed on etched surfaces support that conclusion.

Finally, the performance properties (tensile strength, elongation) were greater with the added plasticizers than with TPS as a second component. The latter case however may be more viable economically. Despite the interest of developing starch/PLA materials, some limitations due to the lack of affinity between respective constituents seem difficult to overcome. The compatibilization of starch and PLA thanks to a copolymer or through reactive blending may be some leads to investigate.

Acknowledgements

This work was funded by Europol'Agro through a research program devoted to the development of packaging materials based on agricultural resources. The authors want to thank Patrice Dole (INRA-Reims, France) for his help with the characterization experiments.

References

[1] Grijpma DW, Pennings AJ. Macromol Chem Phys 1994;195:1649.
[2] Perego G, Cella GD, Bastioli C. J Appl Polym Sci 1996;59:37.
[3] Sinclair RG. J Macromol Sci — Pure Appl Chem 1996;A33:585.
[4] Tsuji H, Ikada Y. J Appl Polym Sci 1998;67:405.
[5] Bigg DM. SPE ANTEC Tech Papers, 1996, 2028.
[6] Lunt J. Polym Degrad Stab 1998;59:145.
[7] Vert M, Schwacch G, Coudane J. J Macromol Sci — Pure Appl Chem 1995;A32:787.

[8] Labrecque LV, Kumar RA, Davé V, Gross RA, McCarthy SP. J Appl Polym Sci 1997;66:1507.
[9] Jacobsen S, Fritz HG. Polym Engng Sci 1996;36:2799.
[10] Jacobsen S, Fritz HG. Polym Engng Sci 1999;39:1303.
[11] Nijenhuis AJ, Colstee E, Grijpma DW, Pennings AJ. Polymer 1996;37:5849.
[12] Ogata N, Jimenez TJ. J Polym Sci, Part B: Polym Phys 1997;35:389.
[13] Zhang L, Goh SH, Lee SY. Polymer 1998;39:4841.
[14] Wang L, Ma W, Gross RA, McCarthy SP. Polym Degrad Stab 1998;59:161.
[15] Grijpma DW, Van Hofslot RDA, Super H, Nijenhuis AJ, Pennings AJ. Polym Engng Sci 1994;34:1674.
[16] Tsuji H, Ikada Y. J Appl Polym Sci 1996;60:2367.
[17] Ma W, McCarthy SP. ANTEC'98; 1998, 2543.
[18] Liu X, Dever M, Fair N, Benson RS. J Environ Polym Degrad 1997;5:225.
[19] Koyama Y, Doi Y. Polymer 1997;38:1589.
[20] Ohkoshi I, Abe H, Doi Y. Polymer 2000;41:5985.
[21] Averous L, Moro L, Dole P, Fringant C. Polymer 2000;41:4157.
[22] Averous L, Fauconnier N, Moro L, Fringant C. J Appl Polym Sci 2000;76:1117.
[23] Knotnis MA, O'Brien GS, Willett JL. J Environ Polym Degrad 1995;3:97.
[24] Bastioli C. Polym Degrad Stab 1998;59:263.
[25] Lörcks J. Polym Degrad Stab 1998;59:245.
[26] Miyata T, Masuko T. Polymer 1998;39:5515.
[27] Cartier L, Okihara T, Ikada Y, Tsuji H, Puiggali J, Lotz B. Polymer 2000;41:8909.
[28] Fisher EW, Sterzel HJ, Wegner G. Polymere 1973;251:980.
[29] Willemse RC, Speijer A, Langeraar AE, Posthuma de Boer A. Polymer 1999;40:6645.
[30] Aubin M, Prud'homme RE. Polym Engng Sci 1988;28:1355.
[31] Schneider HA. Polymer 1989;30:771.
[32] Yu L, Christov V, Christie G, Smyth R, Beh H, Dutt U, Gray J, Harvey T, Do M, Halley P, Lonergan G. Macro'98 37th IUPAC, 1998.
[33] Germain Y, Ernst B, Genelot O, Dhamani C. Soc Rheol 1994;38:681.
[34] Biresaw G, Carriere CJ. Polymer 2000;41:64 (preprints).